Tunable Frequency Division Duplex RF Front-End Using Electrical Balance and Active Cancellation

Leo Laughlin, *Member, IEEE,* Chunqing Zhang, *Member, IEEE,* Mark A. Beach, *Member, IEEE,* Kevin A. Morris, *Member, IEEE,* John L. Haine, *Member, IEEE* Muhammad Kalimuddin Khan, *Member, IEEE,* and Michael McCullagh, *Member, IEEE,*

***Abstract*—This paper presents a novel, tunable, frequency division duplexing RF front-end which combines passive and active self-interference cancellation. An electrical balance duplexer is used to passively cancel transmitter noise in the receive band, and an active canceller is employed to suppress self-interference in the transmit band. Sub-system specifications are developed and a system level analysis of noise and self-interference powers in this novel architecture is provided, thereby illustrating it's operation. A proof-of-concept demonstrator, built from a software defined radio and discrete RF components, has been characterized across a range of duplex configurations in the 700-950 MHz range, and also at 1900 MHz (LTE band 3) and 2600 MHz (LTE band 7). The prototype achieves an impressive 6.0-7.4 dB noise figure in the presence of a +27 dBm LTE uplink Tx blocker for duplex separations of 47.5 MHz and above. The duplexer has also been tested against reference sensitivity testcases defined in the 3GPP LTE specification, demonstrating specification compliant sensitivity in LTE bands 28 (700 MHz), 3 and 7.**

***Index Terms*—Duplexer, Electrical Balance, frequency division duplexing (FDD), in-band full-duplex (IBFD), Self-interference cancellation, tunable filters, 5G mobile communication.**

I. Introduction

TODAY'S cellular handsets achieve frequency division duplex (FDD) operation using fixed-frequency acoustic resonator duplexing filters such as surface acoustic wave (SAW) or bulk acoustic wave devices. These filters are effective in isolating the receiver from the transmit signal, typically providing >50 dB of transmit-to-receive (Tx-Rx) isolation in both the uplink and downlink bands, mitigating the in-band uplink signal and the out-of-band Tx noise, respectively. Supporting multiband operation requires multiple off-chip duplexers, which prohibits covering more than several bands. Because of this, mobile devices currently support only a region specific subset of the >30 FDD bands defined in the 3GPP standards, preventing global roaming on 3GPP long term evolution (LTE), and motivating research into alternative duplexing technologies [1].

Manuscript received 2 Feburary 2018, revised 2 May 2018, accepted 2 June 2018. This research is supported in part by the University of Bristol EPSRC Impact Acceleration Account (EP/K503824/1), in part by the EPSRC SENSE project (EP/P002978/1), and in part by u-blox AG.

L. Laughlin, C. Zhang, M. A. Beach, K. A. Morris, and J. L. Haine are with the Department of Electrical and Electronic Engineering, University of Bristol, BS8 1UB, UK. e-mail: Leo.Laughlin@bristol.ac.uk.

Muhammad Kalimuddin Khan and Michael McCullagh are with u-blox, Lapps Quay, T12 E273, Cork, Co Cork, Ireland.

Color versions of one or more of the figures in this paper are available online at http://ieeexplore.ieee.org

Digital Object Identifier:

In recent years substantial progress has been made toward a fully tunable and reconfigurable radio frequency (RF) front-end [1], [2], but tunable filters which can provide the low insertion loss (IL) and steep roll-off required for FDD remain a distant prospect [3]. Therefore, for duplexing, a variety of novel approaches have been considered. In [4], separate narrowband tunable antennas are used for transmit (Tx) and receive (Rx), however the tuning range and size of the antennas is limiting, and covering all LTE bands may still result in an unacceptable component count. Duplexers based on self-interference cancellation (SIC) have received substantial interest, not only as a potential alternative to filters in FDD applications, but also enabling in-band full-duplex operation (IBFD), which can theoretically double link capacity by allowing simultaneous transmission and reception on the same frequency [5], [6]. Active SIC [7]–[15], in which an additional transmitter is used to actively generate an RF cancellation signal, and passive SIC [16]–[26], wherein the cancellation signal generation is performed through analog signal processing of the RF Tx signal, have both been studied. Electrical balance duplexers (EBDs) [5], [14]–[22], which implement a form of passive SIC, can be implemented on-chip, are tunable over wide frequency ranges, and have demonstrated the power handling, linearity, and low insertion losses required for cellular handset applications [16], [17], [20], [21]. Likewise, tunable integrated active cancellers have also been demonstrated [11]–[13].

In FDD applications, providing isolation simultaneously over both the uplink and downlink bands remains a challenge. In [11]–[13], active SIC is used to cancel Tx leakage, however, even with thermal noise and phase noise suppression mechanisms [13], substantial Rx desensitisation is observed. In [13] the Tx band self-interference (SI) was sufficiently suppressed, but the Rx noise figure was degraded to 15.4 dB at a Tx power of only 17 dBm due to limited cancellation of the Tx noise in the Rx band. Conversely, passive SIC can cancel Tx noise, but wideband cancellation requires high RF complexity. Passive feedforward cancellation requires adaptive multi-tap analog filters [24], [25]. Similarly, in EBDs, the isolation bandwidth is limited by frequency domain variation in the antenna and balancing reflection coefficients, and therefore providing isolation in both bands entails increased RF complexity in the balancing network [18], [20], [27], [28]. Higher order RF processing not only increases the size and cost of the RF front-end, but also requires higher order multidimensional optimisation to tune the circuit parameters [29]–[31]. This may be problematic in mobile device applications where the SI

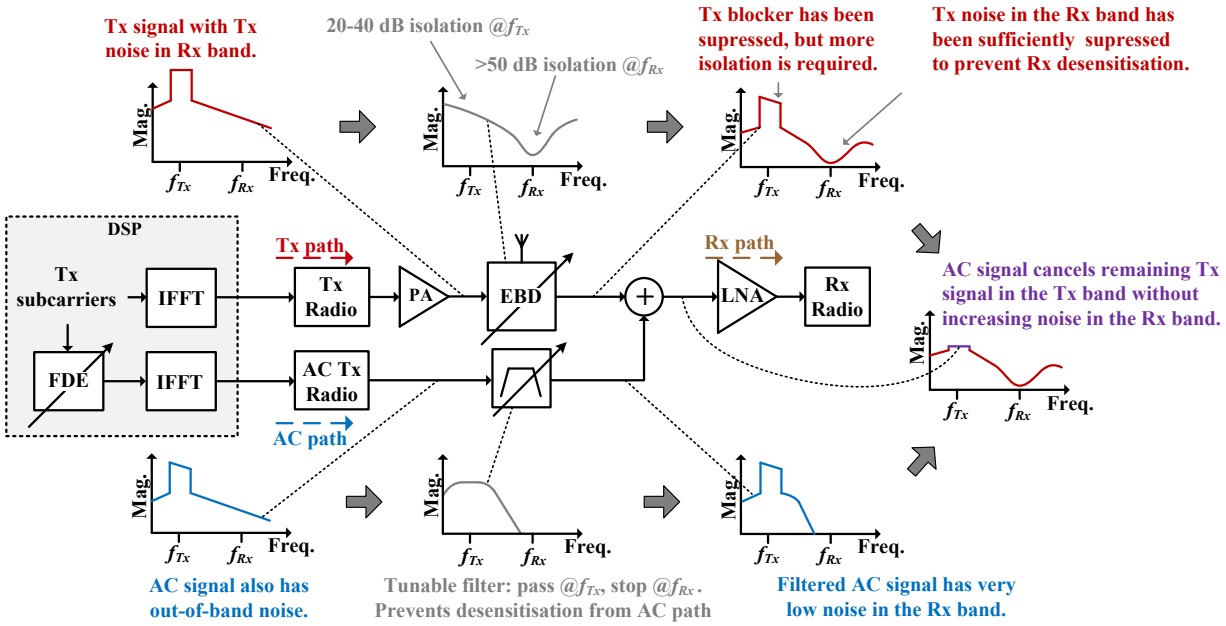

Fig. 1. Block diagram of the proposed electrical balance and active cancellation frequency division duplexer. Also depicted are typical transfer functions and signal spectra at different stages in the architecture, thus illustrating the principle of operation.

channel can be highly dynamic due to interaction between the antenna and environment (e.g. the user's hand/head) [19]. In [22], an EBD, tuned to provide isolation in the downlink band, is combined with a lower performance but tunable SAW filter in the Rx path which attenuates the SI in the uplink band. This was demonstrated to be effective, with the added benefit of blocker rejection, although the drawback of using such a filter in the Rx path is increased Rx IL, and band coverage is limited by the tuning range of the SAW device - this architecture would still require multiple off-chip components to support different frequency ranges.

In this paper we propose a novel frequency division duplexer which combines an EBD with active RF cancellation. This builds on previous works [14], [15], which combined these cancellation techniques for IBFD only. A discrete proof-of-concept demonstrator, which implements an EBD based RF front-end (RFFE) and the necessary baseband processing for active cancellation, has been built and tested. This work also implements a +27 dBm transmitter chain, and characterises the desensitisation in the presence of a full-power LTE uplink Tx blocker. This goes beyond previous works, which either did not characterise desensitisation noise [16]–[18], [20], [22], or did not achieve +27 dBm Tx power [11]–[13]. The architecture was previously presented in [7]; this paper extends [7], providing further qualitative and quantitative system level analysis of the architecture, presenting additional measurement results at different operating frequencies, duplex separations, bandwidths, and power levels, and analyzing desensitization noise coupling mechanisms in the system. The prototype RF front-end has been further developed from [7], integrating the necessary baseband digital signal processing (DSP) to implement a full LTE downlink air interface, and this modem implementation has been tested against the sensitivity testcases defined in the 3GPP LTE specification [32]. The measured sensitivity is comparable to SAW duplexers, passing LTE testcases across a range of operating frequencies, duplex separations, and bandwidths. To the authors' knowledge this is the first tunable frequency division duplexer reported in the literature to demonstrate specification compliant sensitivity.

The remainder of this paper is organized as follows: Section II proposes the novel duplexing architecture, describing the principle of operation and developing sub-system specifications. Section III presents a hardware proof-of-concept, and Section IV provides measured performance. Section V describes the sensitivity testing methodology and results. Section VI concludes.

II. Principle of Operation

A. Electrical balance duplexer

Fig. 1 depicts the proposed electrical balance and active cancellation (EBAC) RFFE. In this design, the EBD is tuned to maximize isolation in the Rx band, mitigating the Tx noise in the Rx band by providing >50 dB of Tx-Rx isolation isolation across the band. However, since the isolation bandwidth of the EBD is limited by the divergent frequency domain trajectories of the antenna and balancing reflection coefficients [5], [14], this level of isolation does not extend to the Tx band; the isolation in this band may typically be only 20-40 dB (depending on the duplex separation).

B. Active canceller

Using the EBD alone, the Tx band isolation is therefore insufficient to prevent receiver overloading, and further Tx band cancellation is required. This is provided by the feed-forward active SI canceller (see Fig. 1). As shown in [8], the active cancellation (AC) signal is generated in the digital baseband domain by processing the Tx waveform. In LTE,

the Tx DSP required for the single carrier frequency division multiple access (SC-FDMA) uplink waveform means that this processing can be readily performed in the frequency domain, using a frequency domain equalizer (FDE) and an additional inverse fast Fourier transform (IFFT) to generate the cancellation waveform. This waveform is then upconverted to RF using the second Tx chain and combined with the received signal, further cancelling the SI in the Tx band. As previously shown [8], [9], [15], this method can compensate for frequency selective amplitude, phase, and delay differences between the self-interference path and the feed-forward path, thereby cancelling SI over wide bandwidths. The dominant limiting factor determining the amount of cancellation is the error vector magnitude (EVM) of the Tx chains. Low cost transceiver hardware has been shown to provide >30 dB of active SIC [9], [33], [34], which is sufficient to increase the isolation in the TX band from as low as 20 dB, to >50 dB, as required.

Various possibilities exist for combining the cancellation signal with the receive signal: a directional coupler can be used in the Rx path prior to the low noise amplifier (LNA), however this adds insertion loss to the Rx and cancellation paths. Other designs could incorporate the interference cancelling LNA proposed in [10], or use the hybrid junction itself to combine the signals, injecting the cancellation signal into the EBD balancing port, as shown in [15]; neither of these methods would increase the Rx IL.

Furthermore, it is notable that both the EBD and AC cancellers will cancel crosstalk between transmitter and receiver components. These cancellation techniques operate upon the aggregate self-interference channel, which may comprise numerous SI coupling mechanisms, and therefore automatically cancel cross-talk as part of normal operation.

C. AC path noise mitigation

Like the main Tx, the AC Tx also generates noise in the Rx band (albeit at a lower power), and if coupled directly to the receiver, this would cause substantial desensitisation. To mitigate this, a tunable filter is inserted in the cancellation path to attenuate the Rx band noise in the cancellation signal in order to avoid this desensitisation. As discussed below, the specification of the tunable filter in the cancellation path is substantially lower than conventional SAW duplexing filters or the tuned Rx path SAW filter used in [22]. This filter may therefore be implemented using alternative (non-acoustic) filter technologies which allow a high level of integration within the radio frequency integrated circuit (RFIC).

D. SI power budget example

Tables I and II give typical values for the SI power and isolation/cancellation at different stages in the duplexing architecture, for the Tx band and Rx band respectively, assuming equal power combining of the Tx and AC signals (e.g. if using an LNA with integrated SI cancellation). This analysis also assumes Tx noise in the Rx band of -129 dBm/Hz at the PA output, and -153 dBm/Hz at the RFIC output, which is typical for LTE user equipment (UE) RF front-ends [4], [35].

TABLE I
DESIGN VALUES FOR SIGNAL POWERS AND LEVELS OF ISOLATION/CANCELLATION IN THE TX BAND.

Tx path		AC path	
PA output	27 dBm	RFIC output stage	7 dBm
EBD isol.	25 dB	Filter IL	5 dB
EBD output.	2 dBm	clc. power	2 dBm
Tx+AC			
SI cancellation		30 dB	
Residual SI		-28 dBm	

TABLE II
DESIGN VALUES FOR NOISE POWERS AND LEVELS OF ISOLATION/ATTENUATION IN THE RX BAND.

Tx path		AC path	
PA noise	-129 dBm/Hz	RFIC noise	-154 dBm/Hz
EBD isol.	50 dB	Filter attn.	25 dB
Rx noise	-179 dBm/Hz	Rx noise	-179 dBm/Hz
Tx+AC+Rx			
desensitisation noise (Tx+AC)		-176.0 dBm/Hz	
LNA thermal noise		-172.0 dBm/Hz (2 dB NF)	
Total noise at LNA (Tx+AC+Rx)		-169.5 dBm/Hz (3.5 dB NF	
Rx IL		3.5 dB	
Antenna referred NF		-166.0 dBm/Hz (7.0 dB NF)	

When tuned to maximize isolation in the Rx band, we may assume the EBD provides around 25 dB of Tx-Rx isolation in the Tx band. When combined with 30 dB of active cancellation, the system provides a total of 55 dB Tx band isolation. For a Tx power of +27 dBm at the PA output, which is 4 dB higher than the LTE maximum transmit power to compensate for the Tx IL from the EBD and interconnects, the residual SI power in the Tx band is -28 dBm, which is sufficiently low to avoid receiver overloading (see Table I). In the AC path, a 5 dB filter IL is assumed, which may result from the relatively steep roll-off required from this filter.

In the Rx band, if the EBD provides 50 dB of Tx-Rx isolation, the noise will be suppressed to -179 dBm/Hz, which is around 7 dB below the LNA thermal noise floor in a typical cellular RFFE, preventing significant desensitisation from the main Tx path. To suppress the Rx band noise from the AC Tx to the same level, the required AC filter stop-band attenuation can be calculated as -154 dBm/Hz $-(-)179$ dBm/Hz = 25 dB. With equal power combining of the Tx and AC signals in the active cancellation process, the sum of the noise from the Tx and AC paths is therefore -176 dBm/Hz. Assuming a 2 dB LNA input noise figure, this equates to 1.5 dB desensitization, to give a desensitized LNA NF of 3.5 dB. Including 3.5 dB of Rx IL from the EBD and interconnects, the antenna referred NF is 7 dB. This example demonstrates that for typical cellular RFFE subsystem specifications, and with an appropriately designed Tx path filter, this duplexing scheme can effectively limit desensitisation from the Tx to acceptable levels for cellular operation. The noise figure could be further reduced by increasing the EBD isolation and filter attenuation specifications. Tx and Rx IL could also be mitigated using noise matched EBDs and a skewed hybrid, as shown in [16], [17].

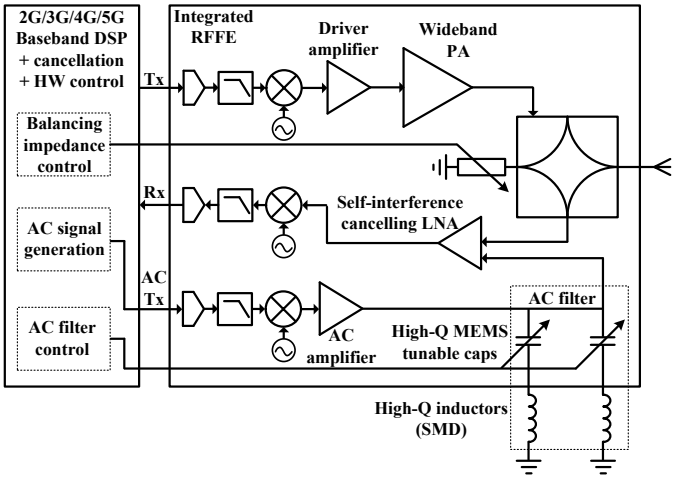

Fig. 2. Possible integrated RFIC implementation based on EBACFDD using integrated high-Q MEMS tunable capacitors and high-Q off-chip inductors for the AC filter, and with active cancellation signal generation and hardware control algorithms implemented in DSP.

E. AC path filter design considerations

Achieving the 25 dB Rx band rejection required in the above example at a narrow duplexing space, e.g., 45 MHz, requires a relatively steep roll-off, however all other design considerations in this application serve to relax the specification of this filter. Firstly, there is no requirement for flatness in the passband: the generation of the AC signal essentially applies inverse filtering to compensate for the transfer function of the AC path (see [36]), and therefore even a large ripple or slope in the passband will not affect the active cancellation. Secondly, since the AC signal power is much lower than the main Tx path, the insertion loss of this filter is not critical to the Tx efficiency, and a substantially higher insertion loss can be tolerated as compared to the conventional duplexing filters currently used in the Tx and Rx path. Thirdly, the instantaneous filter bandwidth requirement is relatively narrow, being at most 20 MHz (for both Tx-band bandpass filter or Rx-band notch filter implementations) which is a 2.5% relative bandwidth at 800 MHz, allowing a relatively selective tunable bandpass/bandstop filter to be applied to achieve a steeper roll off. Achieving adequate noise rejection from the AC path filter is therefore realistic using currently available tunable filtering technologies suitable for integration; for example the micro-electro-mechanical system (MEMS) based tunable filters published in [4] achieve roll-off from 5 dB IL to 25 dB rejection over a relative bandwidth of $<$5%, as required for this application.

An ideal AC path filter would have a tunable range wide enough to cover all bands, however in practice the range will be limited, and therefore, like other front-end components (e.g. PAs, LNAs, mixers), multiple filters may be required to cover multiple ranges (e.g., three filters for low, mid and high frequency ranges).

F. Qualitative comparison

This hybrid passive/active SI cancellation architecture may potentially allow a single RFIC to support FDD operation across wide frequency ranges with just a handful of small off-chip components. An example RFFE implementation is shown in Fig. 2; using the MEMS filter implementation given in [4], this integrated front-end would require just two external high-Q surface mount inductors for the AC path filter.

The requirement for an additional transmit chain does increase the cost, size, and power consumption of the device, however these components can also be implemented on-chip, which is favourable in comparison to discrete alternatives. Furthermore, since the EBD has provided 20-40 dB of Tx-Rx isolation in the Tx band, the cancellation Tx power output is 20-40 dB below the primary Tx power output. Thus, an additional power amplifier (PA) is not required in the cancellation path, and the power consumption of the AC Tx chain is much lower than the primary Tx chain. Consequently, the AC path filter also does not require high power handling capability, and, unlike the main Tx path, achieving low insertion loss in the AC path is not critical to the overall Tx efficiency. However, unlike [22], this design does not provide any blocker rejection from external interferers, and therefore, as is also the case with many other prototypes reported [11]–[13], [16], [17], [21], this duplexer design would require integration with a blocker tolerant receiver. This design increases complexity in the digital baseband domain, requiring additional DSP resources for generating the AC signal, but this is preferable compared to RF domain complexity.

III. HARDWARE PROOF-OF-CONCEPT

Since all of the subsystems in this design have previously been implemented on-chip and have demonstrated the necessary power handling and linearity for cellular applications (e.g., EBDs in [16], [17], [21], active cancellation in [11]–[13], and MEMS tunable filters in [4]), it is clear that integrated circuit implementation of this design is possible. However, rather than fabricating a CMOS prototype to determine on-chip performance, the goal of this work is to experimentally validate the feasibility of the proposed design, prior to embarking on the design of a prototype chip (the function of which also requires system integration with baseband processing, adding substantial complexity to the task). To this end, a proof-of-concept hardware demonstrator was constructed from discrete components and using software definable radio (SDR) test equipment. The various subsystems were designed to have performance which is representative of cellular modem RF front-end sub-systems, and the prototype uses commercial off-the-shelf handset antennas and PAs. Some design choices were made for simplicity of construction (e.g., the use of a directional coupler, as described below), and result in sub-optimal performance compared to that which could be achieved in an optimised design. Therefore, whilst validating the concept of this duplexing scheme, there are further improvements that could be made in future work.

The frequency range of operation of this prototype is determined by the operating ranges of the PAs and filters. This tunable duplexer prototype has been designed for operation in the 700-950 MHz LTE bands. Higher frequency operation is also demonstrated in band 3 (1800 MHz) and band 7 (2600 MHz) using different filters and PAs.

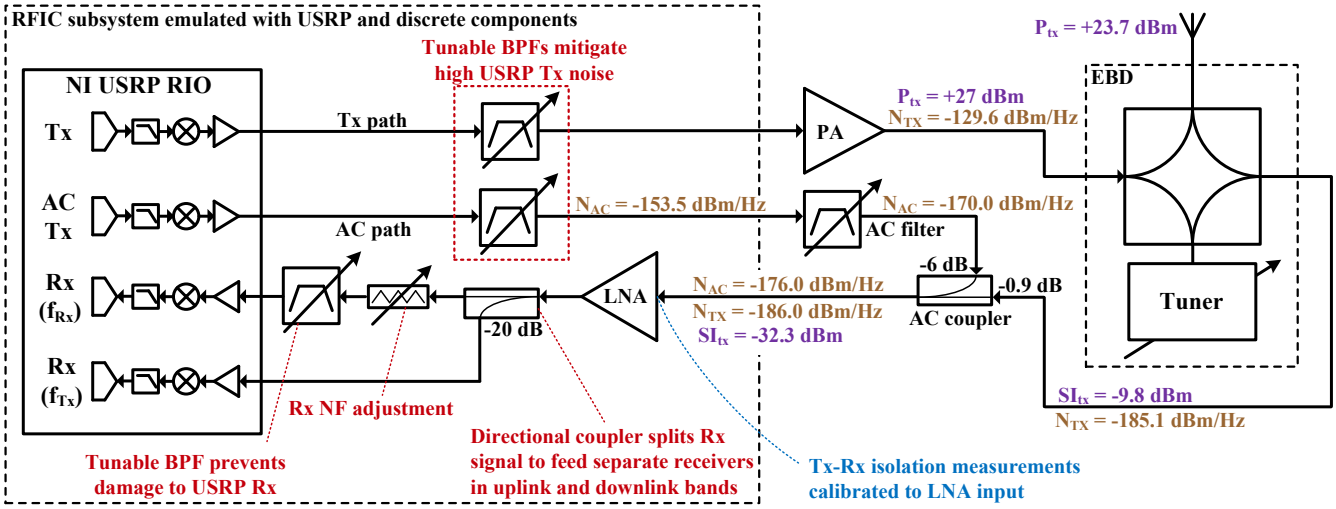

Fig. 3. Block diagram of the hardware proof-of-concept demonstrator. Also indicated are SI powers and noise power spectral densities (PSDs) at different stages in the circuit as measured/inferred for configuration 2 (LTE band 28, see Section IV). N_{AC}=noise PSD due to noise from the AC Tx. N_{TX}=noise PSD due to noise from the primary Tx. P_{Tx}=Tx power. SI_{Tx}=Tx band SI power.

A. Emulated RFIC subsystem

A National Instruments (NI) universal software radio peripheral (USRP) 2942R SDR platform was used for the transmitter and receiver subsystems. This platform provides not only the radio hardware, but also, using LabView, the DSP resources for cancellation signal generation. The USRP does not provide adequate accuracy in Tx output power and measured Rx power; to mitigate this the USRP was benchmarked against a laboratory grade instrument - an NI vector signal transceiver (VST) - and a calibration derived from comparisons with the VST was included in the LabView code controlling the USRP.

The RF performance of the USRP is not representative of a cellular handset RFIC, and additional external components were added in order to emulate RFIC performance. For the transmitter, the Tx noise performance of the USRP is substantially worse than an RFIC: the USRP Tx thermal noise floor is -145 dBm/Hz. This resulted in substantially higher Tx noise at the PA output (-113 dBm/Hz) than would be observed in a cellular RFFE. To mitigate this, tunable filters are required at the USRP Tx outputs. In the Tx path, a tunable pre-PA filter is used, and the Rx band attenuation is adjusted such that the Rx band noise at the PA output is reduced to a representative value of -130 dBm/Hz at a 55 MHz duplex spacing. In the AC path, the filter was tuned such that the Tx noise in the Rx band at the filter output is -153 dBm/Hz, representative of RFIC noise performance. The tunable filter implementations are described in the following sub-section.

The USRP also has a substantially higher noise figure than an RFIC Rx (>7 dB). To mitigate this a Mini-Circuits ZX6083LNS+ LNA was added in the Rx chain. This LNA has a gain of 22 dB and a 1.5 dB noise figure. Since the LNA amplifies the Tx band SI as well as the downlink signal in the Rx band, in this configuration the SI could overload the USRP Rx, even when >50 dB of Tx band isolation is achieved at the LNA input. To prevent damage to the USRP a filter is included between the LNA and the USRP Rx. It is pertinent to note that *this filter does not function as part of the duplexing scheme*[1]; all Tx blocker power (i.e. Tx band SI power) and Rx noise measurements are calibrated to the LNA input, which represents the RFIC Rx input port, and the goal of this experiment is validate the duplexer design by achieving the necessary Tx-Rx isolation *at the LNA input*. An attenuator is also included in the Rx path, allowing the cascaded Rx noise figure to be adjusted by selecting an appropriate attenuation value. The Rx noise figure at the LNA input is set at 2.0-2.1 dB for all experiments. This could be considered typical for LTE modems, and some devices achieve even lower LNA noise figures.

For the USRP-2942R, which has an Rx bandwidth of 40 MHz, is not possible to cover both the uplink and downlink bands with a single receiver. Consequently a separate Rx chain is required for the purpose of running the AC algorithm (which requires measurements of the SI in the Tx band). This Rx is coupled to the receive signal after the LNA using a directional coupler. A -20 dB coupler is used, as this attenuates the Tx band SI sufficiently to prevent overloading of the second USRP Rx.

B. PA, antenna, and cancellation circuitry

The emulated RFIC Tx output (i.e. the filtered USRP Tx output) is connected to an RF micro-devices (RFMD) RF7917 cellular handset PA, mounted on an evaluation board. The PA has a gain of 32 dB and is specified for +27 dBm output power over 699-748 MHz, although in this work it is also used at 887 MHz (configuration 3 as described below), where, for the same level of out-of-band noise, it delivers +23 dBm. The EBD subsystem is implemented using a Krytar model 1831 hybrid coupler, and a Focus electromechanical

[1]Indeed, this filter was not originally included in the experimental setup, and the same results were achieved without damage to the equipment, however due to the potentially high loopback gain from the two amplifiers, this filter was included for equipment safety.

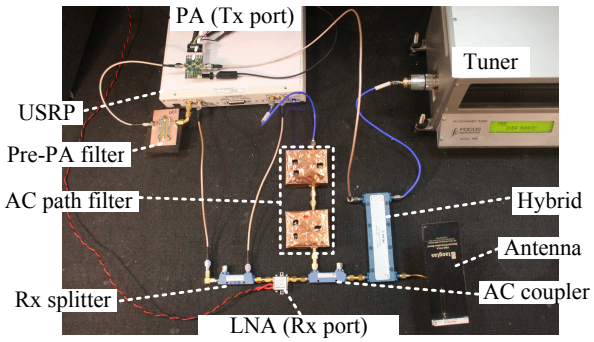

Fig. 4. Photograph of the EBAC FDD demonstrator. Note: during testing the antenna was contained in a shielded enclosure (not shown).

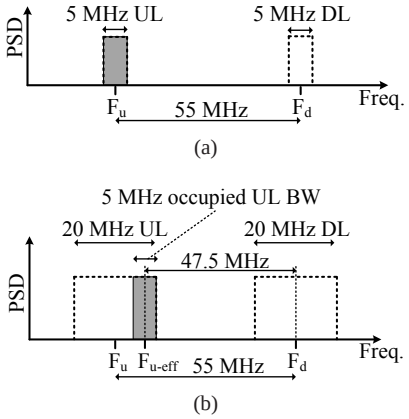

Fig. 5. Frequency division duplex configurations for LTE band 28 sensitivity testcases. (a) 5 MHz downlink testcase. (b) 20 MHz downlink testcase.

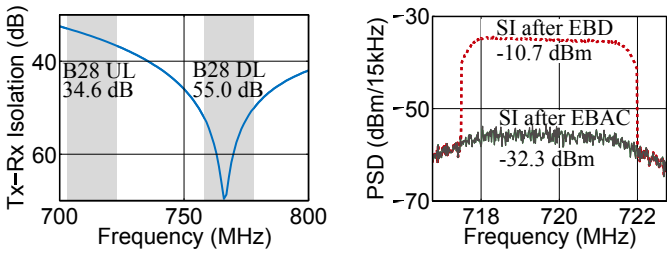

Fig. 6. (a) Measured passive Tx-Rx isolation provided by the EBD. (b) Measured Tx band SI (i.e. the Tx blocker) before and after AC.

impedance tuner. Approximate matching of the group delay of the antenna and tuner was achieved using an appropriate length of transmission line to connect the tuner (this was found to improve isolation in both bands by widening the isolation notch). The hybrid is symmetrical, with approximately 3.1 dB insertion loss in the Tx and Rx paths, and there is 0.2 dB cable loss, and thus a +27 dBm PA output power is sufficient to deliver >+23 dBm at the antenna port, according to the LTE specification. A Taoglas PAD710 is used, this being a typical multiband cellular handset antenna. The antenna was contained within a shielded enclosure lined with radiation absorbent material (RAM); this functioned to prevent emissions in licensed spectrum and interference from external systems. The enclosure was observed to have a small impact on the antenna reflection coefficient, but it was noted that this did not substantially affect the Tx-Rx transfer function of the EBD ($< \pm 1$ dB when correctly balanced), and therefore does not influence the results. The balancing network settings are manually adjusted to achieve high isolation in the Rx band. In practice the same can be achieved using an adaptive EBD balancing algorithm, e.g. [15], [31], however, since the antenna is contained within a static environment, the EBD was not required to be adaptive and manual tuning was sufficient for the purpose of this experiment. The active cancellation FDE coefficients are determined by a zero forcing algorithm as used in [14], [36], utilising the second receiver to measure the SI and AC channels in the Tx band.

The tunable filters in used in this demonstrator are third-order tunable microstrip interdigital filters, manually tuned using mechanically tunable capacitors, and fabricated using FR4. All filters are of the same design, but are tuned to provide different levels of stopband rejection (by tuning the break frequencies). The AC filter Tx band IL is ∼3.5 dB, and the Rx band rejection depends on the duplex separation. The Rx band rejection for LTE band 28 (55 MHz separation) is 24.2 dB. This is representative of the performance achievable using MEMS tunable filters, and is in line with the system level requirements discussed previously (see Tables I and II). The same filter implementation was also used for the filters at the USRP Tx ports, however these filters provide lower stopband rejection of around 9 dB in the AC path and 16 dB in the Tx path. As described above, these filters are used to compensate for high USRP thermal noise and have been tuned to provide representative Rx band noise levels, rather than to maximize Rx band rejection. These filters also add insertion losses of around 3.5 dB.

In the Rx path, the AC signal is coupled using a Mac Technology 3203-6 -6dB directional coupler, which introduces an additional 0.9 dB IL in the Rx path, and 6.0 dB IL in the AC path. This coupling method was chosen for simplicity of implementation in the proof-of-concept demonstrator; as described above in Section II-B there are alternative designs which would avoid these insertion losses. The total Rx IL due to the EBD and directional coupler is 4.0 dB. All connections in this system are sub-miniature version A (SMA). Figs. 3 and 4 respectively depict a block diagram and photograph of the demonstrator.

IV. Measured Performance

A. Duplex configurations

The duplexer has been tested across several duplex configurations as defined for sensitivity testing in the LTE specification [32, Section 7.3]. In many sensitivity testing duplex configurations defined in LTE, the uplink bandwidth is narrower than the downlink bandwidth being tested (see [32, Table 7.3.3-2]). Fig. 5 depicts the duplex configurations defined for downlink sensitivity testing in LTE band 28, for a 5 MHz downlink bandwidth [Fig. 5(a)] and a 20 MHz downlink bandwidth [Fig. 5(b)]. In the 5 MHz downlink testcase the uplink and downlink bandwidths are the same, with a duplexing space of 55 MHz. In the 20 MHz downlink testcase the

TABLE III
MEASURED ISOLATION, NOISE FIGURE, AND SENSITIVITY RESULTS FOR 7 DIFFERENT FDD CONFIGURATIONS. VALUES GIVEN ARE THE AVERAGE OF THE ISOLATION/NOISE ACROSS THE BAND OF INTEREST. NOISE FIGURES ARE REFERRED TO THE ANTENNA PORT.

Configuration parameters	**Config. 1**	**Config. 2**	**Config. 3**	**Config. 4**	**Config. 5**	**Config. 6**	**Config. 7**
LTE band	28	28	N/A	N/A	12	3	7
Uplink centre frequency	713.00 MHz	719.75 MHz	887.75 MHz	719.75 MHz	708.75 MHz	1725.50 MHz	2514.25 MHz
Downlink centre frequency	768.00 MHz	768.00 MHz	936.00 MHz	832.00 MHz	736.00 MHz	1816.00 MHz	2632.00 MHz
Effective Duplex separation	55.00 MHz	48.25 MHz	48.25 MHz	112.25 MHz	27.25 MHz	91.00 MHz	117.75 MHz
Uplink bandwidth	5 MHz	5 MHz	5 MHz	5 MHz	4 MHz	10 MHz	15 MHz
Downlink bandwidth	5 MHz	20 MHz	20 MHz	20 MHz	10 MHz	20 MHz	20 MHz
Measured RF performance							
Rx band isolation (EBD)	58.5 dB	55.9 dB	53.5 dB	56.2 dB	57.0 dB	54.0 dB	52.3 dB
Tx band isolation (EBD)	34.9 dB	37.7 dB	37.1 dB	29.7 dB	39.8 dB	26.3 dB	24.1 dB
Tx band isolation (EBAC)	57.8 dB	59.3 dB	59.0 dB	53.5 dB	61.3 dB	48.8 dB	47.0 dB
Noise figure (Tx NC)	6.0 dB	6.1 dB	6.0 dB	6.0 dB	6.1 dB	6.0 dB	6.0 dB
Noise figure (Tx idle)	6.5 dB	7.1 dB	6.8 dB	6.0 dB	6.3 dB	6.8 dB	6.7 dB
Noise figure (Tx active)	6.9 dB	7.4 dB	6.9 dB	6.0 dB	12.4 dB	7.0 dB	6.8 dB
LTE Sensitivity							
3GPP Specification	-98.5 dBm	-91.0 dBm	N/A	N/A	-94.0 dBm	-91.0 dBm	-92.0 dBm
Measured Sensitivity	-99.5 dBm	-93.1 dBm	-93.6 dBm	-94.6 dBm	-91.4 dBm	-93.7 dBm	-94.9 dBm
Margin	1.0 dB	2.1 dB	N/A	N/A	-2.6 dB	2.7 dB	2.9 dB
Pass/Fail	Pass	Pass	N/A	N/A	Fail	Pass	Pass

uplink bandwidth is only 5 MHz, and the signal occupies the uppermost 5 MHz of the 20 MHz uplink band. This gives a narrower effective duplex separation of 48.25 MHz. In all configurations, the uplink signal is a SC-FDMA waveform, with quadrature phase shift keying (QPSK) modulation, also as defined in the testcases [32].

To demonstrate the performance and tunability of the EBAC duplexer, the prototype has been tested over a range of duplex configurations, as given in Table III. With the exception of configurations 3 and 4, all duplex configurations are exactly as defined for sensitivity testing in LTE bands 28, 12, 3, and 7. Configuration (config) 1 is LTE band 28, 5 MHz downlink bandwidth [Fig. 5(a)] and config 2 is LTE band 28, 20 MHz downlink bandwidth [Fig. 5(b)]. Config 3 is the same as config 2 but with both bands shifted up in frequency to demonstrate tunability. Config 4 has the same uplink configuration as config 2, but the downlink frequency has been shifted up to show performance with a wide duplex separation. Config 5 is LTE band 12, which has an extremely narrow duplex separation of 30 MHz. Configurations 6 and 7 are LTE bands 3 and 7 respectively[2].

B. Results

Fig. 6(a) shows the transfer function of the EBD subsystem as measured on a VNA, with the LTE band 28 uplink and downlink bands indicated, along with the average isolation across these bands. The EBD achieves 55.0 dB isolation in the 20 MHz Rx band, and 34.6 dB across the 20 MHz Tx band. Fig. 6(b) shows the Tx blocker signal measured at the LNA input with and without active cancellation, measured in configuration 2: the 37.7 dB Tx band isolation from the EBD (5 MHz bandwidth) attenuates the 27 dBm Tx signal down to -10.7 dBm the the EBD Rx port, and in this instance the AC provides a further 21.6 dB suppression to increase the isolation to 59.3 dB, which is more than adequate to prevent Rx overloading. Across all configurations AC provided 21-23 dB of suppression. This is limited by RF imperfections in the USRP, and it is expected that higher levels of AC would be achieved with a cellular RFIC transceiver.

Measured results are shown in Table III, which gives the levels of Tx-Rx isolation in the Rx band (as provided by the EBD), and the levels of isolation in the Tx band from the EBD, and when using the EBD and AC (EBAC). Also given are the LNA thermal noise figure as measured with both transmitters not connected (labelled Tx NC), the desensitised noise figure with the transmitters connected and turned on but not transmitting (labelled Tx idle), and the desensitised noise figure when the main Tx is transmitting +27 dBm and the active canceller is running (labelled Tx active). All noise figures are referred to the antenna (i.e. including the 4 dB IL from the EBD and directional coupler).

With the exception of configuration 5, all tested configurations exhibited desensitization of 0.0-1.4 dB, to achieve antenna referred noise figures of 6.0-7.4 dB at downlink bandwidths up to 20 MHz. Configuration 5 achieved significantly higher desensitisation, with the desensitized NF being 12.4 dB. In all configurations the EBD acheives $>$50 dB isolation in the Rx band, and 24-40 dB isolation in the Tx band, with narrower duplex separations having higher Tx band isolation, as would be expected. With the additional Tx band SI suppression from the AC stage, the total Tx band isolation was increased to $>$47 dB in all configurations.

The relatively poor performance in configuration 5 is due to the narrow separation: with 10 MHz uplink and downlink bands and a duplex separation of 30 MHz, there is only a 20 MHz gap between the band edges. In this case the Rx band noise was relatively high due to increased spectral regrowth at the smaller frequency offset, and the AC path filter attenuation

[2]Configurations 1-5 use the same tunable hardware setup. For configurations 6 and 7, in each case the PA and filters were swapped for similar components which provide approximately the same performance at those frequencies. PAs used were RFMD RF7303 and RF7907.

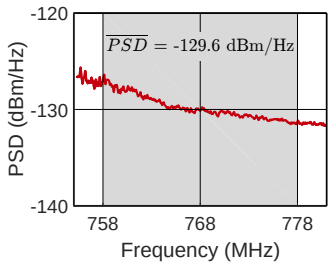

(a) Measured Rx band noise spectrum at the PA output.

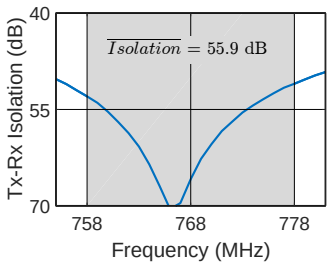

(b) Measured Tx-Rx isolation in the Rx band (EBD isolation + directional coupler IL).

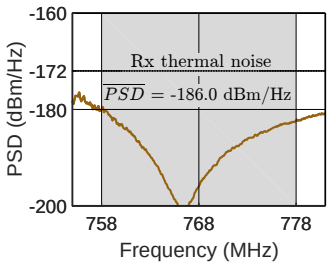

(c) Inferred Tx path desensitization noise spectrum.

Fig. 7. Noise spectra and transfer functions in the Tx-Rx path for the LTE band 28, 20 MHz downlink duplex configuration (configuration 2).

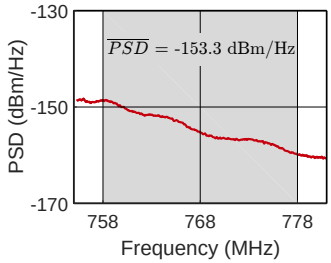

(a) Measured Rx band noise spectrum at the emulated RFIC AC Tx output (i.e. after the first AC filter).

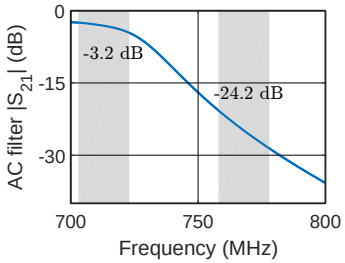

(b) AC path filter transfer function.

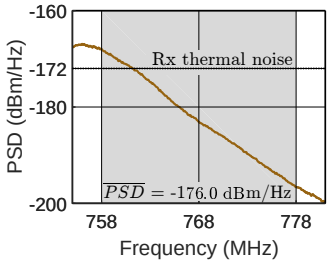

(c) Inferred AC path desensitization noise spectrum.

Fig. 8. Noise spectra and transfer functions in the AC path, measured/inferred for LTE band 28, 20 MHz downlink (configuration 2).

was also lower, resulting in increased desensitisation. This suggests that the EBAC design is not well suited to bands with a very narrow duplex spacing (e.g. 40 MHz and below), and that a better approach for these extremely narrow separations may be to use the EBD only, and tune it to maximize isolation in both bands, rather than in the Rx band. For example, in configuration 5, the EBD requires a 50 dB isolation bandwidth of only 40 MHz in order to concurrently cover the uplink and downlink band. This isolation bandwidth is feasible for an EBD without high RF complexity in the balancing network (e.g. [20]), and providing sufficient isolation in both bands using the EBD would obviate the requirement for AC. For example, in configuration 5 with the AC disabled, no desensitisation was observed, achieving a noise figure of 6.1 dB and almost 40 dB of Tx band isolation from the EBD alone. Conversely, the advantage of the EBAC techniques is clear when observing the performance at the wider duplex separations (e.g. above 40 MHz): in these configurations, covering both bands is potentially infeasible using only an EBD (it would require increased complexity in the balancing network) but instead the AC is effective at increasing the Tx band isolation. Thus this architecture may operate in EBD only mode for very narrow separations, and EBAC mode for wider separations.

C. Quantifying Tx and AC noise sources

Fig. 7 and Fig. 8 provide a detailed analysis of noise coupling in the Tx and AC paths respectively, measured in configuration 2. Fig. 7(a) is the Tx noise in the Rx band at the PA output measured using a spectrum analyzer, and showing an average noise power spectral density (PSD) of -129.6 dBm/Hz. Fig 7(b) is the Tx-Rx transfer function (i.e. the EBD isolation and the directional coupler IL), measured using a VNA, which shows 55.9 dB of Tx-Rx isolation. Fig. 7(c) is the product of the measured spectra in Figs. 7(a) and 7(b). By multiplying these spectra, the desensitisation noise spectrum at the LNA input from the PA output can be inferred (this cannot be directly measured on a spectrum analyzer as it is well below the thermal noise floor of the measurement equipment). In this way, the average Rx band PSD of the desensitisation noise coming from the PA is estimated to be -186.0 dBm/Hz. This is 14 dB below the LNA thermal noise floor, and will therefore cause only slight desensitisation (<0.2 dB in this system).

In the AC path, the first AC path filter is tuned to compensate for the high USRP noise, adjusted such that the average Rx band noise PSD at the emulated RFIC output is -153.3 dBm/Hz, as measured using a spectrum analyzer and shown in Fig. 8(a). Fig. 8(b) shows the transfer function of

TABLE IV
NOISE FIGURE RESULTS WHEN USING TUNABLE AND ACOUSTIC FILTERING IN THE AC PATH.

Tunable AC filter		SAW AC filter	
NF (Tx idle)	NF (Tx active)	NF (Tx idle)	NF (Tx active)
7.1 dB	7.4 dB	6.0 dB	6.1 dB

TABLE V
PERFORMANCE COMPARISON OF DIFFERENT TUNABLE DUPLEXING ARCHITECTURES REPORTED IN THE LITERATURE.

	TMMT '15 [4] Bahramzy et al.	TCAS-I '15 [25] Goel et al.	IMS '17 [26] Khater, Zhou et al.	RFICS '17 [13] Ramakrishnan et al.	TMMT '17 [22] Van Liempd et al.	This work
Architecture	Tunable filters and separate tunable antennas	Tunable filters and passive feedforward SIC	Tunable filters and passive feedforward SIC	Active SIC with noise cancellation	EBD in Rx band and tunable SAW for Tx blocker	EBD in Rx band and active SIC in Tx band
Discrete/integrated	Discrete	Discrete	Discrete	Integrated	Integrated	Discrete
Integration possible	No (antennas)	Yes	No (cavity filters)	Yes	Yes	Yes
FDD and/or IBFD	FDD only	FDD only	FDD only	FDD and IBFD	FDD and IBFD	FDD and IBFD
Frequency range	1710-2170 MHz	700-984 MHz	860-1030 MHz	1000-2000 MHz	700-1000 MHz	700-946 MHz[d]
Tx IL	0 dB[a]	4.6-8.5 dB	not reported	0 dB[c]	2.6-3.4 dB	3.1 dB
Rx IL	2.8-3.4 dB[a]	4.0-7.7 dB	1.6-2.2 dB	not reported	not reported	4.0 dB
Tx band isol. BW)	65 dB (20MHz)	>50 dB (10MHz)	>45 dB (2MHz)	64 dB	>50 dB (10MHz)	>47 dB (20MHz)
Rx band isol. (BW)	50 dB (20MHz)	>50 dB (10MHz)	25-30 dB (20MHz)	not reported	>50 dB (2MHz)	>50 dB (20MHz)
Rx NF (ant.)	4.8-5.4 dB[a]	5.4 dB[b]	not reported	3.6 dB[c]	7.6-8.9 dB	6.0-6.1 dB
Tx power (ant.)	not reported	17 dBm	not reported	17 dBm[c]	24 dBm	23.9 dBm
Desens. NF (ant.)	not reported	8.0 dB[b]	not reported	15.4 dB[c]	not reported	6.0-7.4[e]

[a] Does not include losses in antenna tuner; [b] Cascaded Rx NF calculated from [25, Fig. 17] and assuming a 2 dB LNA NF. Other tuning setting will be several dB worse due to higher IL; [c] Does not include transformer losses. [d] Also measured at 1900 and 2700 MHz; [e] Duplex separation >45 MHz.

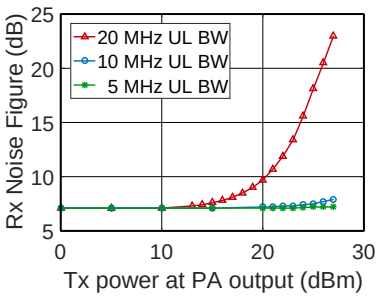

Fig. 9. Measured noise figure in a 20 MHz downlink bandwidth for different transmit powers, for 5 MHz, 10 MHz and 20 MHz uplink bandwidths. LTE band 28, duplex separation: 55 MHz. The 20 MHz uplink bandwidth results in substantial desensitization at higher Tx powers, however this configuration is not included in LTE sensitivity testing.

the second AC path filter as measured on a VNA: The filter provides an average rejection of 24.2 dB of across the Rx band and an average Tx band insertion loss of 3.2 dB. Fig. 8(c) is the inferred desensitisation noise spectrum at the LNA input coming from the AC path. This is calculated by multiplying the measured noise spectrum at the USRP output and the transfer function of the full AC path (the two AC filters and the directional coupler measured together in series using a VNA). The average Rx band PSD of the desensitisation noise coming from the AC path is thereby estimated as -176.0 dBm/Hz. This is much larger than the desensitisation noise coming from the PA, and comparable to the LNA thermal noise, and is therefore the dominant cause of the desensitisation.

The final desensitised NF can be predicted by adding the measured LNA thermal noise power to the inferred desensitisation noise powers of the two desensitisation sources. In this way the desensitized NF is calculated as 7.6 dB. This agrees well with the measured NF in configuration 2 of 7.4 dB. Fig. 3 is also annotated with measured and inferred noise and SI power levels at different points in the circuit (as measured/calculated for configuration 2).

To further demonstrate that the AC path is the dominant desensitisation source the AC path filter was replaced with an LTE band 28 Tx SAW filter (the Tx path of a TDK B8538 duplexer), which can suppress the noise from the AC by >50 dB, rendering it insignificant compared to the other noise sources. Table IV compares the measured noise figures when using the SAW AC filter vs the tunable AC filter: the desensitisation is reduced from 1.4 dB with the tunable AC filter, to 0.1 dB with the SAW AC filter. This is further evidence that the AC path noise is the dominant source of desensitization in this implementation, and shows that increasing the noise rejection in the AC path will reduce desensitization, as would be expected.

D. Wider Tx bandwidths

Configurations 1-7 are based on duplex configurations defined for sensitivity testing in the LTE specification. In all of these configurations the uplink bandwidth is narrower than the downlink bandwidth, which serves to relax the testcase by reducing the Rx band noise from spectral regrowth in the PA. To investigate the performance of the EBAC duplexer without this form of relaxation, the desensitized noise figure has also been measured for uplink bandwidths up to 20 MHz, for a range of Tx power levels. Measurements were performed for LTE band 28, with a downlink bandwidth of 20 MHz and a duplex separation of 55 MHz (i.e. configuration 2), for uplink bandwidths of 5, 10, and 20 MHz, and Tx powers of 0-27 dBm.

Fig. 9 plots the measured desensitized noise figure in these configurations. For the 5 and 10 MHz uplink bandwidths, desensitization is minimal, but for the 20 MHz uplink bandwidth, desensitization is severe, with a NF of 23 dB being measured at maximum Tx power. However, for the 20 MHz uplink bandwidth, substantial desensitization is only observed for Tx powers above 15 dBm, and the EBAC duplexer functions well below this power level. Although this demonstrates a clear limitation in the performance of this duplexer (the lower Rx band isolation can result in desensitisation), in a real network deployment a UE is unlikely to be allocated a 20 MHz

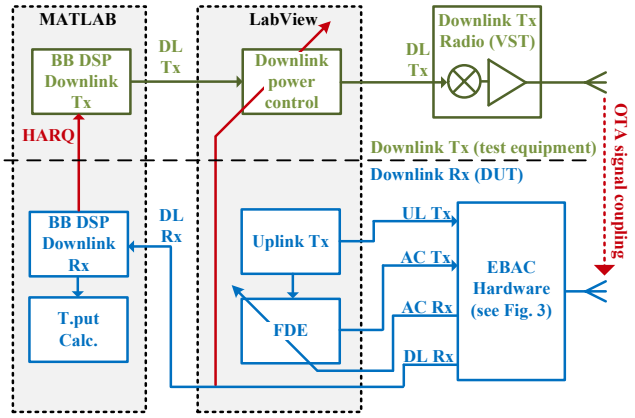

Fig. 10. Block diagram of software and hardware subsystems in the throughput sensitivity test. T.put=throughput.

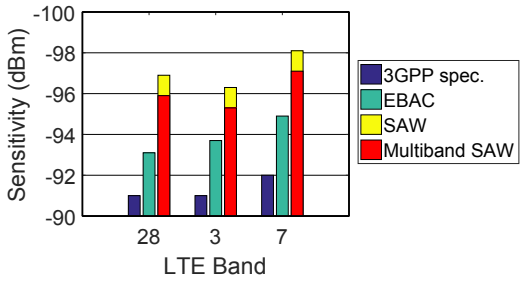

Fig. 11. Comparison of sensitivity testing requirements and measured sensitivity for EBAC and SAW duplexers.

uplink bandwidth at full transmit power. Therefore, despite this shortcoming, the performance of the duplexer can still be considered satisfactory.

E. Performnce comparison

Table V compares this work with alternative architectures which have been presented in the literature. The Tx/Rx bandwidth achieved in this work is only matched by [4], however this architecture relies on tunable antennas with a very limited frequency range. This work outperforms all other architectures in terms of desensitized noise figure, however this discrete prototype is not directly comparable to the integrated prototypes [13], [22] and further work is required to determine the performance of this architecture in an RFIC implementation.

V. LTE SENSITIVITY TESTING

In order to assess the viability of this duplexing architecture in LTE UE applications, and assess the impact of the desensitisation noise on downlink throughput, the EBAC prototype has been tested according to the downlink sensitivity test-cases defined in the LTE specification [32, Section 7.3]. This is especially relevant to this design given the spectrally inconsistent nature of the desensitisation noise (see Fig. 8c), as this noise will have a disproportionate impact on some subcarriers over others, which may lead to greater downlink throughput degradation compared to white noise of the same power. The LTE UE sensitivity testcases are defined in terms of downlink throughput, with the device under test (DUT) required to achieve $>$95% of the maximum throughput in a specified physical layer configuration at or below a given downlink receive power. Therefore, performing this testcase requires the downlink physical layer modem signal processing and data-link layer functions [e.g., synchronization, error control coding, and hybrid automatic repeat request (HARQ)] to be implemented and interfaced with the EBAC hardware.

Here, MATLAB was used to implement the necessary physical layer and data-link layer downlink processing, utilizing the LTE system toolbox, which provides all of the necessary code required for a downlink throughput test-case. The MATLAB signal processing code is interfaced with LabView using the MATLAB script node which allows LabView to make calls to MATLAB code. This vastly reduced the workload compared to implementing the entire LTE downlink air interface in LabView.

The sensitivity testing setup is depicted in Fig. 10. LTE reference sensitivity power levels are defined with reference to the antenna port: closed loop power control and appropriate calibrations are applied in order to control the receive power at this point in the circuit. Downlink Tx waveforms are generated in MATLAB, and the downlink Tx IQ is passed to Labview, where the power control is applied. The downlink signal is upconverted to RF and transmitted over-the-air (OTA) using an NI vector signal transceiver (VST), coupled to the downlink Tx antenna through a -30 dB attenuator. The downlink transmitting antenna and the DUT antenna are contained within the same shielded enclosure, which, as previously described, prevents unlicensed emissions and interference from external sources. This enclosure is lined with RAM and there is limited multipath propagation between the antennas; this satisfies the requirement for a static frequency-flat downlink channel as defined in the testcase.

The downlink signal is received through the EBAC front-end hardware, which functions as previously described Section III, and the Rx baseband IQ is passed from LabView to further MATLAB functions which perform all baseband Rx DSP (i.e. synchronisation, demodulation, error control). The LTE downlink channel requires HARQ feedback in the uplink direction. In this demonstrator the uplink portion of the air interface is not implemented, and the HARQ information is passed directly from the receiver processing to the transmitter processing in software. Since the downlink sensitivity testcases define error free uplink feedback this simplification is congruent with the specification. The system processes downlink waveforms one sub-frame at a time. Due to processing delays in MATLAB, the air-interface does not conform to the timing requirements of LTE (the processing delay is larger than the sub-frame period), however this has no impact on the sensitivity measurement result.

Sensitivity testing was performed for configurations 1-7, and results are given in Table III, which also provides the 3GPP sensitivity requirement and the pass/fail margin (where applicable). The duplexer passes all sensitivity testcases except for configuration 5, with pass margins of 1.0-2.9 dB, demonstrating the suitability of this design for duplexing in LTE.

For purpose of comparison, the sensitivity tests were also repeated in bands 28, 3, and 7 (20 MHz downlink bandwidths), using commercial SAW duplexers (TDK B8538, Epcos B8808, and Epcos B8089) in place of the EBAC duplexer. Fig. 11 compares the measured sensitivity when using the SAW and EBAC duplexers, along with the 3GPP reference sensitivity requirement for these bands. It is pertinent to note that for multi-band SAW based RFFEs, there is additional insertion loss from the switching and routing circuitry - for comparison this is also included in Fig. 11 by assuming a 1 dB IL for the switching/routing, and adding this to the measured SAW sensitivity value. In all cases the SAW duplexers outperform the EBAC duplexer, even with the additional IL. However, the EBAC results are comparable, and comfortably exceed the 3GPP sensitivity requirements.

VI. Conclusion

This paper has presented a novel frequency division duplexer which combines an electrical balance duplexer with an active RF self-interference canceller. A proof of concept demonstrator has been implemented using a software definable radio platform and discrete RF hardware, implementing the RF front-end and baseband processing for this hybrid passive/active cancellation architecture.

The RF performance of the duplexer has been characterized across a range of frequencies and duplex separations, including measurements of the desensitized noise figure in the presence of a full power LTE Tx blocker. The prototype achieves a 6.0-7.4 dB desensitized noise figure for duplex separations of 47.5 MHz and above. Furthermore, the duplexer has been integrated within a full LTE downlink air interface, and tested according to sensitivity testcases as defined in the LTE specification. Specification compliant sensitivity has been demonstrated in LTE bands 28, 3, and 7, showing performance comparable to SAW duplexers.

The EBAC prototype performs poorly at very narrow duplex separations, achieving a 12.4 dB NF in LTE band 12 (30 MHz duplex separation), and failing the sensitivity testcase for this band. This indicates that the EBAC is not suitable for very narrow duplex separations (e.g. below 40 MHz) due to limited filtering of noise in the AC path. However for these scenarios it is feasible that the EBD isolation bandwidth is sufficiently wide to cover the uplink and downlink bands, meaning that this architecture could operate at very narrow duplex separations simply by disabling the active canceller.

Whilst sub-system specifications and overall performance may differ between this discrete SDR based prototype and an integrated implementation, this work has successfully demonstrated system level integration of these passive and active cancellation techniques for FDD applications. This work has proven the viability of this novel design, opening a new avenue in the pursuit of an integrated tunable RF front-end. Further work is required to investigate variant designs which could mitigate insertion losses using improved cancellation signal coupling methods and asymmetric hybrids with noise matched LNAs, and to determine the performance of this architecture in an integrated circuit implementation

Acknowledgments

The Authors would like to thank colleagues at u-blox Cork and u-blox Cambourne, in particular B. Swaminathan, R. O'Leary, P. Herczog, J. Connelly, S. Lu, and A. Normanton, for their support. The Authors also thank E. Arabi for his advice, K. Stevens for building the tunable filters, and Taoglas, TDK/Epcos, and RFMD/Qorvo for providing components used in this work.

References

[1] J. Tsutsumi, *et al.*, "Cost-Efficient, High-Volume Transmission: Advanced Transmission Design and Architecture of Next Generation RF Modems and Front-Ends," *IEEE Microw. Mag.*, vol. 16, no. 7, pp. 26–45, aug 2015.

[2] L. Larson, "RF and Microwave Hardware Challenges for Future Radio Spectrum Access," *Proc. IEEE*, vol. 102, no. 3, pp. 321–333, mar 2014.

[3] R. Aigner, "Tunable Filters? Reality Check! Foreseeable Trends in System Architecture for Tunable RF Filters," *IEEE Microw. Mag.*, vol. 16, no. 7, pp. 82–88, aug 2015.

[4] P. Bahramzy, *et al.*, "A Tunable RF Front-End With Narrowband Antennas for Mobile Devices," *IEEE Trans. Microw. Theory Techn.*, vol. 63, no. 10, pp. 3300–3310, oct 2015.

[5] L. Laughlin, *et al.*, "Optimum Single Antenna Full Duplex Using Hybrid Junctions," *IEEE J. Sel. Areas Commun.*, vol. 32, no. 9, pp. 1653–1661, sep 2014.

[6] A. Sabharwal, *et al.*, "In-Band Full-Duplex Wireless: Challenges and Opportunities," *IEEE J. Sel. Areas Commun.*, vol. 32, no. 9, pp. 1637–1652, sep 2014.

[7] L. Laughlin, *et al.*, "A 700-950 MHz Tunable Frequency Division Duplex Transceiver Combining Passive and Active Self-interference Cancellation," in *2018 IEEE MTT-S Int. Microw. Symp.*, Philadelphia, PA. USA., 2018, pp. 1–4.

[8] A. Sahai, G. Patel, and A. Sabharwal, "Pushing the limits of full duplex wireless: design and real-time implementation," Rice Univ. Houston, TX, Tech. Rep. TREE1104, 2011. [Online]. Available: http://arxiv.org/abs/1107.0607

[9] E. Everett, A. Sahai, and A. Sabharwal, "Passive Self-Interference Suppression for Full-Duplex Infrastructure Nodes," *Wirel. Commun. IEEE Trans.*, vol. 13, no. 2, pp. 680–694, 2014.

[10] J. Zhou, *et al.*, "Low-Noise Active Cancellation of Transmitter Leakage and Transmitter Noise in Broadband Wireless Receivers for FDD/Co-Existence," *IEEE J. Solid-State Circuits*, vol. 49, no. 12, pp. 3046–3062, dec 2014.

[11] S. Ramakrishnan, *et al.*, "A 65nm CMOS transceiver with integrated active cancellation supporting FDD from 1GHz to 1.8GHz at +12.6dBm TX power leakage," in *2016 IEEE Symp. VLSI Circuits*. IEEE, jun 2016, pp. 1–2.

[12] L. Calderin, *et al.*, "Analysis and Design of Integrated Active Cancellation Transceiver for Frequency Division Duplex Systems," *IEEE J. Solid-State Circuits*, vol. 52, no. 8, pp. 2038–2054, aug 2017.

[13] S. Ramakrishnan, *et al.*, "An FD/FDD transceiver with RX band thermal, quantization, and phase noise rejection and >64dB TX signal cancellation," in *2017 IEEE Radio Freq. Integr. Circuits Symp.* IEEE, jun 2017, pp. 352–355.

[14] L. Laughlin, *et al.*, "A Widely Tunable Full Duplex Transceiver Combining Electrical Balance Isolation and Active Analog Cancellation," in *2015 IEEE 81st Veh. Technol. Conf. (VTC Spring)*. IEEE, may 2015, pp. 1–5.

[15] ——, "Passive and Active Electrical Balance Duplexers," *IEEE Trans. Circuits Syst. II Express Briefs*, vol. 63, no. 1, pp. 94–98, jan 2016.

[16] M. Mikhemar, H. Darabi, and A. A. Abidi, "A Multiband RF Antenna Duplexer on CMOS: Design and Performance," *Solid-State Circuits, IEEE J.*, vol. 48, no. 9, pp. 2067–2077, 2013.

[17] S. H. Abdelhalem, P. S. Gudem, and L. E. Larson, "Hybrid Transformer-Based Tunable Differential Duplexer in a 90-nm CMOS Process," *Microw. Theory Tech. IEEE Trans.*, vol. 61, no. 3, pp. 1316–1326, 2013.

[18] ——, "Tunable CMOS Integrated Duplexer With Antenna Impedance Tracking and High Isolation in the Transmit and Receive Bands," *IEEE Trans. Microw. Theory Techn.*, vol. 62, no. 9, pp. 2092–2104, sep 2014.

[19] L. Laughlin, *et al.*, "Electrical balance duplexing for small form factor realization of in-band full duplex," *IEEE Commun. Mag.*, vol. 53, no. 5, pp. 102–110, may 2015.

[20] B. van Liempd, *et al.*, "A Dual-Notch +27dBm Tx-Power Electrical-Balance Duplexer," in *ESSCIRC 2014 - 40th Eur. Solid State Circuits Conf.* IEEE, sep 2014, pp. 463–466.
[21] ——, "A +70-dBm IIP3 Electrical-Balance Duplexer for Highly Integrated Tunable Front-Ends," *IEEE Trans. Microw. Theory Techn.*, pp. 1–13, 2016.
[22] ——, "Adaptive RF Front-Ends Using Electrical-Balance Duplexers and Tuned SAW Resonators," *IEEE Trans. Microw. Theory Techn.*, pp. 1–8, 2017.
[23] D. Bharadia, E. McMilin, and S. Katti, "Full Duplex Radios," in *Proc. 2013 ACM SIGCOMM*, Hong Kong, 2013.
[24] J. Zhou, *et al.*, "Integrated Wideband Self-Interference Cancellation in the RF Domain for FDD and Full-Duplex Wireless," *IEEE J. Solid-State Circuits*, vol. 50, no. 12, pp. 3015–3031, dec 2015.
[25] A. Goel, B. Analui, and H. Hashemi, "Tunable Duplexer With Passive Feed-Forward Cancellation to Improve the RX-TX Isolation," *IEEE Trans. Circuits Syst. I Regul. Pap.*, vol. 62, no. 2, pp. 536–544, feb 2015.
[26] M. A. Khater, *et al.*, "A tunable 0.861.03 GHz FDD wireless communication system with an evanescent-mode diplexer and a self-interference-cancelling receiver," in *2017 IEEE MTT-S Int. Microw. Symp.* IEEE, jun 2017, pp. 376–379.
[27] E. Manuzzato, *et al.*, "Digitally-Controlled Electrical Balance Duplexer for Transmitter-Receiver Isolation in Full-Duplex Radio," in *Eur. Wirel. Conf.*, 2016.
[28] B. Hershberg, *et al.*, "20.8 A dual-frequency 0.7-to-1GHz balance network for electrical balance duplexers," in *2016 IEEE Int. Solid-State Circuits Conf.* IEEE, jan 2016, pp. 356–357.
[29] M. Mikhael, *et al.*, "A Full-Duplex Transceiver Prototype with In-System Automated Tuning of the RF Self-Interference Cancellation," in *Proc. 1st Int. Conf. 5G Ubiquitous Connect.* ICST, 2014, pp. 110–115.
[30] T. Vermeulen, *et al.*, "Real-time RF self-interference cancellation for in-band full duplex," in *2015 IEEE Int. Symp. Dyn. Spectr. Access Networks*. IEEE, sep 2015, pp. 275–276.
[31] G. Castellano, *et al.*, "A low power control system for real-time tuning of a hybrid transformer-based receiver," in *2016 IEEE Int. Conf. Electron. Circuits Syst.* IEEE, dec 2016, pp. 328–331.
[32] 3GPP, "Evolved Universal Terrestrial Radio Access (E-UTRA); User Equipment (UE) conformance specification; Radio transmission and reception. Part 1: Conformance Testing," 3rd Generation Partnership Project (3GPP), TS 36.521-1 v14.4.0, 09 2017.
[33] M. Duarte and A. Sabharwal, "Full-duplex wireless communications using off-the-shelf radios: Feasibility and first results," in *Signals, Syst. Comput. (ASILOMAR), 2010 Conf. Rec. Forty Fourth Asilomar Conf.*, 2010, pp. 1558–1562.
[34] M. Duarte, C. Dick, and A. Sabharwal, "Experiment-Driven Characterization of Full-Duplex Wireless Systems," *IEEE Trans. Wirel. Commun.*, vol. 11, no. 12, pp. 4296–4307, dec 2012.
[35] RFMD, "RF7917 LTE Band 12/17/28 Linear PA Module," RF Micro Devices (RFMD), Datasheet DS20140520, 2013.
[36] W. Schacherbauer, *et al.*, "An Interference Cancellation Technique for the Use in Multiband Software Radio Frontend Design," in *Microw. Conf. 2000. 30th Eur.*, 2000, pp. 1–4.

Leo Laughlin received the M.Eng. degree in Electronic Engineering from the University of York, York, U.K., in 2011, and the Ph.D degree in Communications Engineering from the University of Bristol, Bristol, U.K., in 2016. In 2009-10 he was at Qualcomm in Farnborough, U.K., working on Physical Layer DSP for GSM receivers. In 2011 he was at Omnisense Ltd in Cambridge, working on radio geolocation systems. He is currently a Research Fellow in the Communications Systems and Networks Laboratory at the University of Bristol. His research interests are in tunable and reconfigurable radio technologies for mobile devices.

Chunqing Zhang was awarded the M.Sc. degree in Telecommunication and Information Systems from Beijing Jiaotong University, Beijing, China, in 2004. Between 2004 and 2014 he worked in the R&D department and the Testing department of Datang-Mobile Telecommunication Equipment Co. LTD., Beijing, China. Since 2014 he has been a Ph.D student and Research Assistant in the Communication Systems and Networks Laboratory, University of Bristol, Bristol, U.K.

Mark A. Beach received his PhD for research addressing the application of Smart Antenna techniques to GPS from the University of Bristol in 1989, where he subsequently joined as a member of academic staff. He was promoted to Senior Lecturer in 1996, Reader in 1998 and Professor in 2003. He was Head of the Department of Electrical and Electronic Engineering from 2006 to 2010, and then spearheaded Bristols hosting of the EPSRC Centre for Doctoral Training (CDT) in Communications. He currently manages the delivery of the CDT in Communications, leads research in the field of enabling technologies for the delivery of 5G and beyond wireless connectivity, as well as his role as the School Research Impact Director. Mark's current research activities are delivered through the Communication Systems and Networks Group, forming a key component within Bristol's Smart Internet Lab. He has over 25 years of physical layer wireless research embracing the application of Spread Spectrum technology for cellular systems, adaptive or smart antenna for capacity and range extension in wireless networks and MIMO aided connectivity for through-put enhancement. Millimetre Wave technologies as well as flexible RF technologies for SDR modems underpin his current research portfolio.

Kevin A. Morris received the B.Eng. and Ph.D. degrees in electronics and communications engineering from the University of Bristol, Bristol, U.K., in 1995 and 2000, respectively. He is currently a Reader of RF engineering and Head of the Department of Electrical and Electronic Engineering, University of Bristol. He has authored or co-authored 90 academic papers and he holds five patents. His research interests principally concern looking at methods of reducing power consumption in communications systems including the area of RF hardware design with a specific interest in the design of efficient linear broadband power amplifiers for use within future communications systems. Dr. Morris is currently involved with a number of the Engineering and Physical Sciences Research Council (EPSRC) research programmes including FARAD and SENSE and industry funded research programmes within the U.K. He is a member of the UK Electronic Skills Foundation (UK-ESF) Strategic Advisory board.

John L. Haine is Royal Academy of Engineering Professor in Electrical and Electronic Engineering at the University of Bristol. He graduated with B.Sc (1971) and Ph.D (1977) degrees from Birmingham and Leeds Universities in the UK. He has worked on wireless R&D for a number of companies including start-ups, focusing mainly on air interface and circuit aspects, as well as being involved in a number of standards and M&A activities. He is retired from u-blox AG, where he worked on new standards for IoT communications and key cellular RF implementation technologies. He is a Life Member of the IEEE, and serves on the boards of Cambridge Wireless and the IoT Security Foundation.

Michael McCullagh is the Receiver Lead RF Engineer in the u-blox cellular RFIC group. In recent years his main focus has been on designing RF/analogue blocks in bulk CMOS for IoT, V2X and LTE cellular applications. Prior to this role, he has designed and delivered RFICs for GPS/GLONASS, digital and analogue broadcast (DAB, DVB, FM), UWB (15.4a), WiFi, Bluetooth, various cellular (GSM, WCDMA), mm-wave back-haul and optical communications in CMOS, BiCMOS and III-V based technologies. He has also worked on Power Amplifier (cellular and radar), integrated duplexer (EBI) and RF front-end module design. He has published extensively and filed patents relating to cellular, UWB and navigation. He has a BEng (1st class) in Electrical and Electronic Engineering and an MSc (with distinction) in Microwaves and Optoelectronics from University College London.

Muhammad Kalimuddin Khan is RF system architect at the u-blox cellular RFIC group Cork, Ireland and a visiting industrial fellow at the University of Bristol, UK. His main focus and interest recently has been on the calibration algorithms, interference cancellation in duplexing technologies and digitally/FW assist RF for LTE cellular, short range applications. Previously he worked at Analog devices, Cork, Ireland on low power RF IC transceiver development as mixed signal control loop designer for wireless sensor network, smart metering, and home automation applications etc. He has published extensively and hold numerous patents in RF transceiver topics. He holds PhD degree in electronics engineering from Newcastle university, UK and B.Eng. (Electrical Eng,) from NED university, Karachi, Pakistan.